nature genetics

Loss of BBS proteins causes anosmia in humans and defects in olfactory cilia structure and function in the mouse

Heather M Kulaga[1], Carmen C Leitch[2], Erica R Eichers[3], Jose L Badano[2], Alysa Lesemann[1], Bethan E Hoskins[4], James R Lupski[3,5,6], Philip L Beales[4], Randall R Reed[1] & Nicholas Katsanis[2,7]

Defects in cilia are associated with several human disorders, including Kartagener syndrome[1], polycystic kidney disease[2,3], nephronophthisis[4] and hydrocephalus[5]. We proposed that the pleiotropic phenotype of Bardet-Biedl syndrome (BBS), which encompasses retinal degeneration, truncal obesity, renal and limb malformations and developmental delay, is due to dysfunction of basal bodies and cilia[6,7]. Here we show that individuals with BBS have partial or complete anosmia. To test whether this phenotype is caused by ciliary defects of olfactory sensory neurons, we examined mice with deletions of *Bbs1* or *Bbs4*. Loss of function of either BBS protein affected the olfactory, but not the respiratory, epithelium, causing severe reduction of the ciliated border, disorganization of the dendritic microtubule network and trapping of olfactory ciliary proteins in dendrites and cell bodies. Our data indicate that BBS proteins have a role in the microtubule organization of mammalian ciliated cells and that anosmia might be a useful determinant of other pleiotropic disorders with a suspected ciliary involvement.

BBS is caused by mutations in at least eight loci, seven of which have been identified[6,8–14]. Although the sequences of the BBS proteins have not provided any clues to their function, BBS4, BBS5 and BBS8 are localized to the basal body of cultured cells and at ciliated borders in tissues[6,7,10]. In addition, all known orthologs of the mammalian BBS proteins are expressed specifically in ciliated sensory neurons in *Caenorhabditis elegans*[6,10], raising the possibility that disruption of these proteins will lead to ciliary defects.

Although the capacity to generate cilia is shared by most mammalian cells, some cells develop specialized cilia that mediate sensory function. The olfactory receptor neuron is a highly specialized example of a ciliated cell in which the apical process terminates in a complex structure, the dendritic knob, containing multiple basal bodies[15]. Eight or more immotile cilia emanate from this dendritic knob and extend more than 60 μm into the mucus. Given that at least three BBS proteins localize to the olfactory epithelium[6,7], we considered that if ciliary defects underlie BBS, then olfactory structure and sensory function should be compromised in individuals with BBS. To test this hypothesis, we evaluated 19 individuals with BBS from 14 unrelated families using the fully validated, 12-item smell identification test. To compensate for varying degrees of visual impairment in subjects, each test was administered in a controlled setting by the same personnel. The test has a maximum possible score of 12. We compared the score of each individual with sex-derived normative data, ranked the relative degree of olfactory function by percentile and categorized olfactory function as normal (score of 9–12), abnormal (score of 8) or

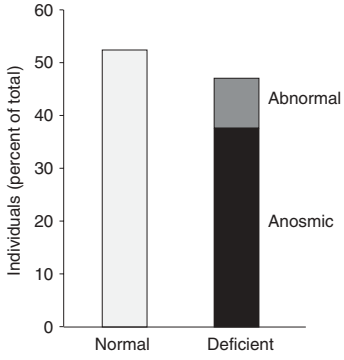

Figure 1 Olfactory phenotypes of individuals with BBS. Nineteen individuals (median age = 24 years, age range = 7–49 y; nine males, seven females) diagnosed with BBS were evaluated with the B-SIT olfactory function test. Ten individuals, including all three <15 y of age, scored in the normal range (9–12). Two subjects were abnormal (score of 8), and seven scored in the anosmic range (≤7).

[1]Howard Hughes Medical Institute and Department of Molecular Biology and Genetics, and [2]Institute of Genetic Medicine, 533 Broadway Street Building, Johns Hopkins University, 733 N. Broadway, Baltimore, Maryland 21205, USA. [3]Department of Molecular and Human Genetics, Baylor College of Medicine, Houston, Texas 77030, USA. [4]Molecular Medicine Unit, Institute of Child Health, University College London, London WC1 1EH, UK. [5]Department of Pediatrics and [6]The Texas Children's Hospital, Baylor College of Medicine, Houston, Texas 77030, USA. [7]Wilmer Eye Institute, Johns Hopkins University, Baltimore, Maryland 21287, USA. Correspondence should be addressed to N.K. (katsanis@jhmi.edu).

Published online 22 August 2004; doi:10.1038/ng1418

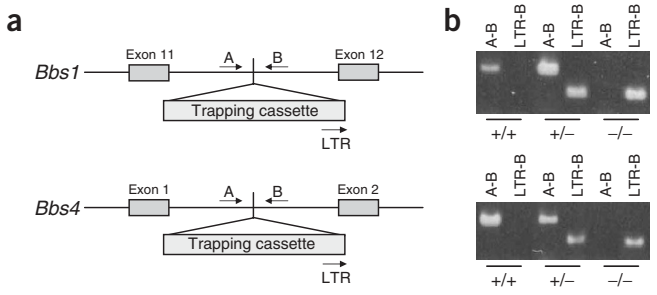

Figure 2 Insertional targeting of *Bbs1* and *Bbs4*. (**a**) Partial representation of the *Bbs1* and *Bbs4* genomic regions, indicating the sites of insertion of the trapping cassettes. Exons and vector are depicted as gray boxes. Arrows labeled A, B and LTR indicate the location of the primers used for PCR-based genotyping. (**b**) Two different PCRs were carried out to genotype each line (*Bbs1*, upper panel; *Bbs4*, lower panel; genotypes given beneath panels): A-B amplifies a ~500-bp region from the wild-type chromosome, whereas LTR-B detects the insertional event by amplifying a ~300-bp fragment.

anosmic (score of 1–7; ref. 16). Forty-seven percent of individuals with BBS were completely or partially anosmic (**Fig. 1**). Seven of these 19 individuals (37%) had scores in the range of 3–7, and another two individuals (10%) had intermediate scores (**Supplementary Table 1** online). Notably, four of the six individuals who were homozygous with respect to a mutation causing the amino acid substitution M390R in BBS1, the most common BBS-associated mutation in individuals of European descent[13,17], had scores in the normal range. This result is consistent with the hypothesis that mutations in additional loci can modify the expressivity of the phenotype[10,17,18]. Notably, all three individuals with null mutations in *BBS8* whom we tested had normal olfaction. Detailed phenotypic analysis of all the individuals with BBS whom we studied did not identify any correlation with other specific features (**Supplementary Table 1** online).

These data suggested that olfaction is severely compromised in some individuals with BBS. Recurrent otitis media and sinusitis are also associated with BBS[19]. Although none of the subjects showed evidence of an upper respiratory tract infection on the day of test administration, we could not rule out the possibility that some other form of chronic nasal congestion might confound the results. To resolve this issue and to address the molecular mechanisms underlying these presumed sensory cilia defects, we analyzed the structure and function of the olfactory and adjacent respiratory nasal epithelium in mice with ablation of *Bbs1* or *Bbs4*. We disrupted the genes by inserting a gene-trapping cassette into intron 11 (*Bbs1*) or intron 1 (*Bbs4*; **Fig. 2a**), which resulted in aberrant splicing and complete loss of the mRNA message, as determined by RT-PCR (data not shown). We bred mice to homozygosity, determined genotypes by PCR (**Fig. 2b**) and confirmed them by Southern blotting (data not shown). Both mouse lines had skewed mendelian ratios, with 40–50% embryonic lethality evident by embryonic day 10.5 as partially reabsorbed embryos. Consistent with an oligogenic causality model[18,20], *Bbs1*-null and *Bbs4*-null mice had considerable phenotypic

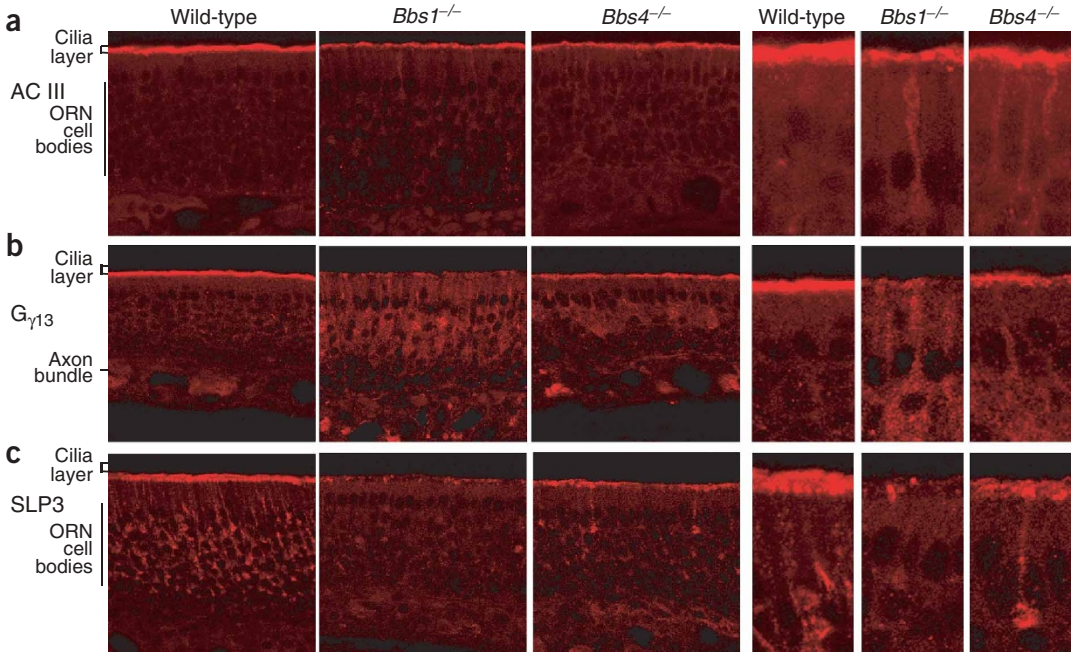

Figure 3 Defects in olfactory protein localization in *Bbs1*$^{-/-}$ and *Bbs4*$^{-/-}$ mice. Sections of olfactory epithelium were immunostained with antibodies to olfactory cilia-enriched signal transduction components (AC III and $G_{\gamma 13}$) and to the dendrite, dendritic knob and cilia protein SLP3. (**a**) AC III is enriched in the cilia layer of wild-type mice. Staining is less intense in olfactory epithelium of *Bbs1*$^{-/-}$ and *Bbs4*$^{-/-}$ mice. A fraction of the AC III seems to be trapped in the dendritic processes of null mice. This pattern is more apparent in the adjacent higher-magnification images of the olfactory epithelium from mice of each genotype. (**b**) $G_{\gamma 13}$ is largely absent in the cilia layer of *Bbs1*$^{-/-}$ and *Bbs4*$^{-/-}$ mice. Considerable $G_{\gamma 13}$ accumulates in the neuronal cell bodies. Staining of $G_{\gamma 13}$ in axon bundles is essentially unaffected. (**c**) SLP3 is concentrated in the dendrites and the dendritic knobs on the luminal surface of the olfactory epithelium. In *Bbs1*$^{-/-}$ and *Bbs4*$^{-/-}$ mice, staining in these structure is markedly reduced. Images are ~1-μm optical confocal sections acquired from similar regions of the olfactory septum. ORN, olfactory receptor neuron.

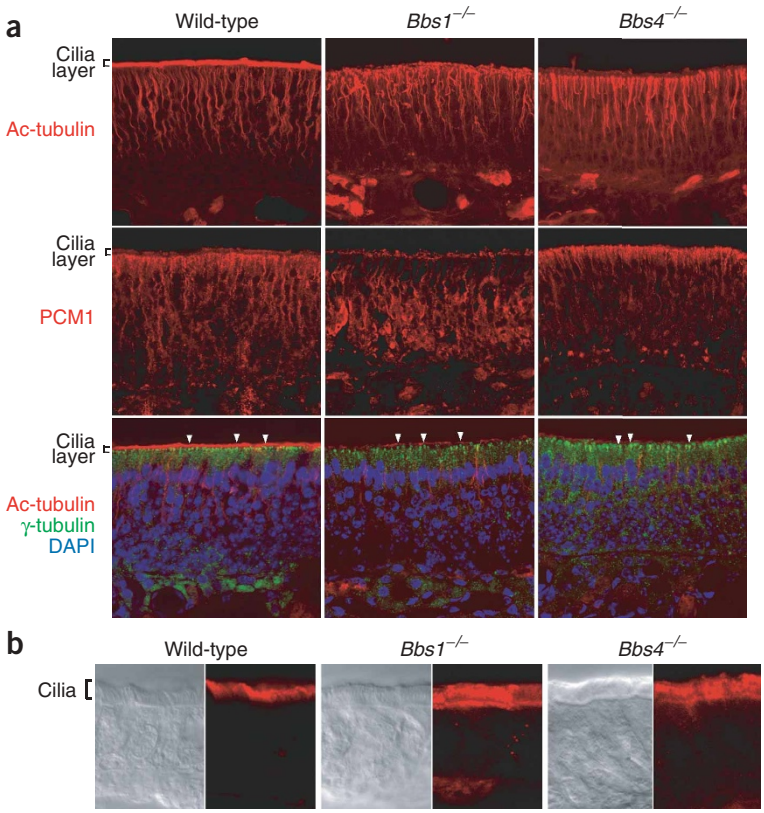

Figure 4 Microtubule organization in epithelium of *Bbs1*$^{-/-}$ and *Bbs4*$^{-/-}$ mice. (**a**) Intense staining for acetylated α-tubulin in the cilia layer of the olfactory epithelium is observed in wild-type mice but is essentially absent in *Bbs1*$^{-/-}$ and *Bbs4*$^{-/-}$ mice. The dendrites extending from the neuronal nucleus to the luminal surface are intact but disorganized, which correlates with trapped PCM1 in the cell body (in *Bbs1*$^{-/-}$ mice) or the dendritic knob (in *Bbs4*$^{-/-}$ mice). In triple-fluorophore images, γ-tubulin (green) labels basal bodies (arrows) and acetylated α-tubulin marks the cilia layer in olfactory epithelium of wild-type mice and short cilia in null mice. Single-fluorophor images are presented as a single image flattened from a 20-μm stack of 1-μm optical sections to allow visualization of many dendrites. Triple-labeled images are ~1-μm optical confocal sections that result in better detection of basal bodies containing γ-tubulin. (**b**) Regions of respiratory epithelium adjacent to olfactory tissue have normal cilia in wild-type, *Bbs1*$^{-/-}$ and *Bbs4*$^{-/-}$ mice. The left panel for each genotype is a DIC image and the right panel is the same area visualized with an antibody to acetylated α-tubulin. Images are ~1-μm optical confocal sections.

variability. None of the null mice had polydactyly, renal and liver malformations or situs inversus. All null mice were runts at birth (weighing 30–50% less than littermates); by week 10, ~10% of the mice became obese and 30% developed retinal degeneration.

We first investigated whether the distribution of cilia-enriched olfactory proteins was disrupted in *Bbs1*$^{-/-}$ or *Bbs4*$^{-/-}$ mice. Type III adenylyl cyclase (AC III), essential for odorant signaling[21], is enriched in olfactory cilia[22]. Immunostaining with an antibody specific for AC III yielded the expected intense staining in the ciliary layer in wild-type mice but markedly lower signal intensity in olfactory epithelium of *Bbs1*$^{-/-}$ or *Bbs4*$^{-/-}$ mice (**Fig. 3a**). We observed AC III–specific staining in the apical dendrites of null mice but never in dendrites of wild-type mice (**Fig. 3a**). A second signal-transduction protein enriched in olfactory sensory cilia, $G_{\gamma 13}$, was essentially absent from the cilia of *Bbs1*$^{-/-}$ mice and substantially less abundant in *Bbs4*$^{-/-}$ mice, but the intensity of $G_{\gamma 13}$ staining in the axon bundles that underlie the basal lamina in each case was similar to that of wild-type controls. $G_{\gamma 13}$ immunoreactivity was substantially higher in the cell bodies and dendrites of olfactory neurons of olfactory epithelium of *Bbs1*$^{-/-}$ and *Bbs4*$^{-/-}$ mice than in olfactory epithelium of wild-type mice (**Fig. 3b**).

The olfactory-specific lipid-raft protein SLP3 is restricted to the apical dendrite and cilia of olfactory receptor neurons and may be involved in ciliogenesis and trafficking of transduction components to their apical site of action[23]. In olfactory epithelium of *Bbs1*$^{-/-}$ and *Bbs4*$^{-/-}$ mice, SLP3 was depleted from the cilia layer and adjacent dendritic knobs (**Fig. 3c**). Notably, the protein seems to be down-regulated markedly in null mice. We occasionally observed cells with SLP3 staining, which may be new neurons that are continually replaced in this tissue[24].

The absence of AC III, $G_{\gamma 13}$ and SLP3 in the cilia of null mice could result from a specific defect in the localization of these proteins or could reflect a failure of olfactory epithelium in *Bbs1*$^{-/-}$ or *Bbs4*$^{-/-}$ mice to fully develop cilia. To distinguish between these possibilities, we examined the integrity of structural cilia components by staining coronal sections of the nasal epithelium with antibodies to acetylated α-tubulin. Unlike wild-type mice, which showed prominent staining distal to the dendritic knob, olfactory cilia of null mice were depleted of stable microtubules (**Fig. 4a**) and the ciliary layer was markedly thinner. In addition, whereas the microtubule bundles in the dendrites of olfactory neurons in wild-type mice were straight apical projections to the luminal surface, *Bbs1*$^{-/-}$ and *Bbs4*$^{-/-}$ mice had distorted apical dendrites. Notably, PCM1, a protein that requires BBS4 to organize microtubule radiation *in vitro*[7], was also mislocalized in null mice. In *Bbs1*$^{-/-}$ mice, PCM1 was trapped in the neuronal cell body and correlated with a disorganized microtubular dendritic network, whereas in *Bbs4*$^{-/-}$ mice, PCM1 was restricted to the dendritic knobs, which correlated with shorter dendritic microtubule bundles (**Fig. 4a**).

To examine the integrity of the dendritic knobs, we investigated the localization of γ-tubulin, a specific basal body marker. γ-tubulin staining was indistinguishable in dendritic knobs of *Bbs1*$^{-/-}$, *Bbs4*$^{-/-}$ and wild-type mice (**Fig. 4a**), suggesting that the observed distortions in the dendrites do not derive from an absence of the basal bodies. Finally, we examined the adjacent respiratory epithelium to assess the status of the cilia. The respiratory epithelium had a robust cilia layer and intense staining with acetylated α-tubulin, indicating that the respiratory epithelial cells are nearly normal in the null mice (**Fig. 4b**). Taken together, these results indicate that loss of BBS1 or BBS4 protein results in the near elimination of structural and nonstructural cilia components from the apical surface and, at most, only short axonemal cilia remain to transduce sensory information.

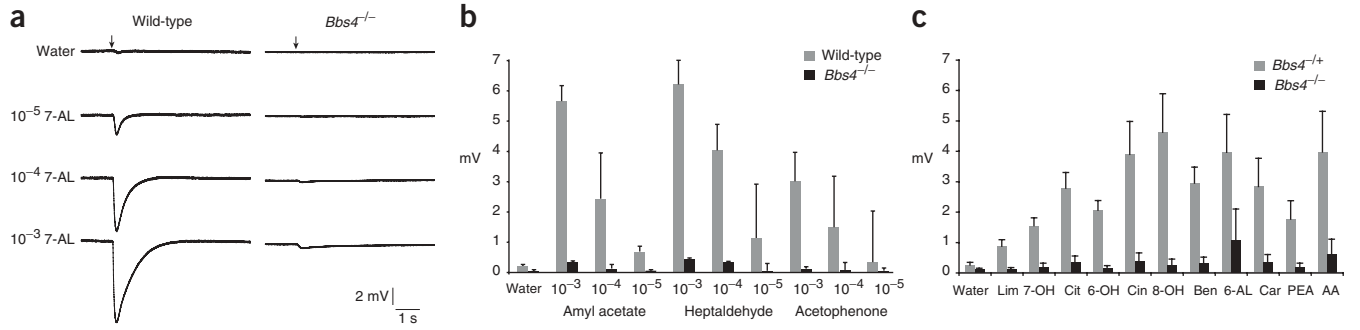

Figure 5 Olfactory responses of *Bbs4*$^{-/-}$ mice. The olfactory epithelia of adult wild-type and *Bbs4*$^{-/-}$ mice were exposed to a brief pulse (60 ms; arrows) of vapor-phase odorants and EOGs were recorded. (**a**) Representative EOG traces upon exposure to water or dilute solutions of heptaldehyde (7-AL). (**b**) Graphical representation of responses in olfactory epithelium of wild-type and *Bbs4*$^{-/-}$ mice. Three odorants were examined over a three-log range of odor concentration. Although a dose-dependent response was observed for both genotypes, the responses of *Bbs4*$^{-/-}$ mice were much smaller than those of wild-type littermates. Data shown are mean ± s.d. of four independent recordings from three wild-type mice and five independent recordings from three *Bbs4*$^{-/-}$ mice. Concentrations are given in molar units. (**c**) Ten additional odorants were examined at a concentration of 10^{-4} M. Data shown are mean ± s.d. of four (*Bbs4*$^{-/+}$) or six (*Bbs4*$^{-/-}$) independent recordings from three mice. All experiments in **c** were done without knowledge of genotype. Wat, water; Lim, limonene; 7-OH, heptanol; Cit, citronellal; 6-OH, hexanol; Cin, cineol; 8-OH, octanol; Ben, benzaldeyde; 6-AL, hexanal; Car, carvone; PEA, phenyl ethyl alcohol; AA, amyl acetate.

Given their histological phenotypes, *Bbs1*$^{-/-}$ and *Bbs4*$^{-/-}$ mice are predicted to be anosmic. To test this prediction directly, we examined the ability of the olfactory epithelium from *Bbs4*$^{-/-}$ mice to respond to odorant stimuli, because it seems to retain modest concentrations of correctly localized AC III, $G_{\gamma 13}$ and SLP3 compared with that of *Bbs1*$^{-/-}$ mice (**Fig. 3**). We applied odorants as brief pulses to the olfactory epithelium of wild-type and *Bbs4*$^{-/-}$ mice while recording an electroolfactogram (EOG), the summated generator potential of the sensory neurons, from the mucosal surface. Wild-type mice produced large (5–9 mV), dose-dependent responses to the odorant heptaldehyde. In contrast, *Bbs4*$^{-/-}$ mice had only nominal responses, even at the highest odor concentration (**Fig. 5a**). We obtained similar results for each of the odorants tested (**Fig. 5b**). We also tested *Bbs4*$^{-/-}$ and *Bbs4*$^{+/-}$ mice with a structurally diverse collection of odorants at a single concentration that minimized desensitization and confirmed that the observed olfactory defects extended to many odors (**Fig. 5c**). We conclude that the structural defects in cilia and apical dendrites leads to a functional loss (or severe impairment) of olfactory function. Our results correlate the psychophysically determined anosmias in individuals with BBS with specific electrophysiological and cellular defects in the mouse model.

Our studies show that anosmia is a new clinical manifestation of BBS and that loss of function of BBS1 and BBS4 leads to structural and functional defects in the mouse olfactory epithelium. These data support the hypothesis that ciliary defects underlie the pleiotropic BBS phenotype[6]. Our previous *in vitro* studies also indicated that suppression of *BBS4* mRNA caused marked disorganization of centrosomal microtubules[7]. The observed phenotype of *Bbs1*$^{-/-}$ and *Bbs4*$^{-/-}$ mice indicates that such disorganization affects two discrete structures. The organization of the ciliary axoneme is severely disrupted, with little or no stable microtubules in the olfactory cilia, and the microtubular organization of dendrites is also distorted, though not completely abolished. These data suggest that loss of BBS protein function inhibits both intraflagellar transport, the motor-mediated movement of particles along ciliary axonemes[25], and microtubule-dependent transport in the cytoplasm of dendrites. Notably, the distribution of several ciliary proteins is perturbed in *Bbs1*$^{-/-}$ and *Bbs4*$^{-/-}$ mice, but the degree to which they are mislocalized varies. These observations suggest that there might be multiple transport mechanisms to the ciliary axoneme, some of which are directly affected by microtubule disorganization.

Our data also suggest that testing for anosmia might be a useful diagnostic screen for BBS and other ciliary diseases. The association of hypogonadotrophic hypogonadism and anosmia constitutes X-linked Kallmann syndrome (OMIM 308700). *KAL1* encodes a protein, anosmin, that has a key role in the migration of neurons expressing gonadotropin-releasing hormone and olfactory nerves to the hypothalamus[26]. Moreover, anosmia has been reported in individuals with various neurological disorders, including Alzheimer disease and Huntington disease[27]. Although this might be a secondary manifestation of other defects in the central nervous system, at least one of the huntingtin-interacting proteins, CHE13 (ref. 28), is a component of intraflagellar transport in *C. elegans*[29]. Given the mechanistic overlap between intraflagellar transport and dendritic transport[30] and the phenotype of the olfactory dendrites of *Bbs1*$^{-/-}$ and *Bbs4*$^{-/-}$ mice, we propose that physiological, functional and structural studies of olfactory sensory neurons might provide insights into dendritic function in other neuronal cells.

METHODS

Individuals with BBS. We collated clinical data, carried out clinical examinations and diagnosed BBS according to established criteria. We obtained blood and clinical data with consent, in accordance with protocols approved by the human subjects ethics committees at each participating institution. We administered Scratch and Sniff Brief Smell Identification Test booklets (Sensonics) in accordance with the manufacturer's instructions. The tests were done in the same room on the same day and administered by the same personnel to standardize environmental variables. To control for visual impairment, we read the possible responses out loud and allowed the subject to choose one odor in response.

***Bbs1*$^{-/-}$ and *Bbs4*$^{-/-}$ mice.** We targeted 129SvEvAB2.2 embryonic stem cell lines for *Bbs1* and *Bbs4* in accordance with established protocols and with a protocol approved by the Animal Care and Usage Committees at the participating institutions. We confirmed the insertion by Southern blotting and amplification and sequencing from the insertion cassette. We microinjected 20 mouse embryonic stem cells into host blastocysts according to standard methods. We bred chimeras to C57BL/6J mice, which were then bred to homozygosity. We carried out genotyping using locus-specific primers for *Bbs1* and *Bbs4*, as well as cassette-specific primers, and confirmed genotypes by Southern blotting. We

extracted RNA with the Trizol reagent from dissected hearts and kidneys of *Bbs1* and *Bbs4* heterozygotes and mutant homozygotes and carried out RT-PCR using gene-specific primers[6]. Primer sequences are available on request. All analyses were done on a 1:1 129:BL6 background.

Antibodies and immunohistochemistry. We anesthetized mice with ketamine-xylazine (RBI), perfused them intracardially with phosphate-buffered saline and isolated fixed tissues. For cryosections, we treated dissected tissues with 30% sucrose plus 250 mM EDTA for 24 h at 4 °C, froze them in OCT compound (Sukura Finetek) and cut sections (20 μm) in a cryostat.

We analyzed immunohistochemistry on adult olfactory tissue sections fixed in Bouin's. We washed sections in buffer T (0.1 M Tris (pH 7.5), 0.15 M NaCl, 0.1% Tween 20) three times for 5 min each before incubating them in buffer T plus 10% normal serum (buffer T1). We diluted the primary antibody in buffer T1 and incubated sections at 20 °C for 1 h. We used primary antibodies at the following dilutions: AC III at 1:1,000 (Santa Cruz), $G_{\gamma 13}$ at 1:500 (A.L. and R.R.R., unpublished data), SLP3 at 1:1,000 (ref. 25) and rabbit acetylated α-tubulin at 1:1,000 (Sigma). We washed sections in Buffer T three times for 5 min each at room temperature and visualized antibody binding with a Cy3-conjugated secondary antibody. We mounted coverslips in antifade reagent (Vector Laboratories). For triple-staining experiments, we used a polyclonal antibody to γ-tubulin at 1:500 (Sigma) and a monoclonal antibody to acetylated α-tubulin at 1:1,000 (Sigma) and visualized them with Alexa488 (Molecular Probes) or Cy3 fluorophore (Jackson Laboratories). We visualized nuclei with the DNA stain DAPI. All images were collected on a Zeiss LSM 510 in multitrack mode.

EOG recordings. We generated vapor-phase odor stimuli by placing 2 ml of solution in a sealed 10-ml glass test tube. We delivered vapor as a 60-ms pulse injected into a continuous stream of humidified air flowing over the tissue sample. We occasionally used two electrodes, placed on either turbinate IIb or turbinate III, to acquire simultaneous recordings from a mouse. We analyzed data with Clampfit (Axon Instruments) and determined peak heights from prepulse baseline, but did no other data normalizations. All odorants were purchased from Aldrich.

Note: Supplementary information is available on the Nature Genetics website.

ACKNOWLEDGMENTS

We thank the individuals with BBS and their families for their continued support; M. Leroux and S. Houston for critical evaluation of the manuscript; and J. Hill, A. Ross and H. May-Simera for technical assistance. This study was supported in part by grants from National Institute of Child Health and Development, National Institutes of Health (N.K.); the March of Dimes (N.K. and J.R.L.); the National Institute of Deafness and Other Communication Disorders, National Institutes of Health (R.R.R.); the National Kidney Research Fund (B.E.H.); and the Wellcome Trust (P.L.B.). P.L.B. is a Wellcome Trust Senior Research Fellow. R.R.R. is a Howard Hughes Investigator.

COMPETING INTERESTS STATEMENT

The authors declare that they have no competing financial interests.

Received 31 May; accepted 2 August 2004
Published online at http://www.nature.com/naturegenetics/

1. Afzelius, B.A. A human syndrome caused by immotile cilia. *Science* **193**, 317–319 (1976).
2. Pazour, G.J. *et al.* Chlamydomonas IFT88 and its mouse homologue, polycystic kidney disease gene tg737, are required for assembly of cilia and flagella. *J. Cell Biol.* **151**, 709–718 (2000).
3. Nauli, S.M. *et al.* Polycystins 1 and 2 mediate mechanosensation in the primary cilium of kidney cells. *Nat. Genet.* **33**, 129–137 (2003).
4. Otto, E.A. *et al.* Mutations in INVS encoding inversin cause nephronophthisis type 2, linking renal cystic disease to the function of primary cilia and left-right axis determination. *Nat. Genet.* **34**, 413–420 (2003).
5. Chen, J., Knowles, H.J., Hebert, J.L. & Hackett, B.P. Mutation of the mouse hepatocyte nuclear factor/forkhead homologue 4 gene results in an absence of cilia and random left-right asymmetry. *J. Clin. Invest.* **102**, 1077–1082 (1998).
6. Ansley, S.J. *et al.* Basal body dysfunction is a likely cause of pleiotropic Bardet-Biedl syndrome. *Nature* **425**, 628–633 (2003).
7. Kim, J.C. *et al.* The Bardet-Biedl protein BBS4 targets cargo to the pericentriolar region and is required for microtubule anchoring and cell cycle progression. *Nat. Genet.* **36**, 462–470 (2004).
8. Badano, J.L. *et al.* Identification of a novel Bardet-Biedl syndrome protein, BBS7, that shares structural features with BBS1 and BBS2. *Am. J. Hum. Genet.* **72**, 650–658 (2003).
9. Katsanis, N. *et al.* Mutations in MKKS cause obesity, retinal dystrophy and renal malformations associated with Bardet-Biedl syndrome. *Nat. Genet.* **26**, 67–70 (2000).
10. Li, J.B. *et al.* Comparative genomics identifies a flagellar and basal body proteome that includes the BBS5 human disease gene. *Cell* **117**, 541–552 (2004).
11. Slavotinek, A.M. *et al.* Mutations in MKKS cause Bardet-Biedl syndrome. *Nat. Genet.* **26**, 15–16 (2000).
12. Nishimura, D.Y. *et al.* Positional cloning of a novel gene on chromosome 16q causing Bardet-Biedl syndrome (BBS2). *Hum. Mol. Genet.* **10**, 865–874 (2001).
13. Mykytyn, K. *et al.* Identification of the gene (*BBS1*) most commonly involved in Bardet-Biedl syndrome, a complex human obesity syndrome. *Nat. Genet.* **31**, 435–438 (2002).
14. Mykytyn, K. *et al.* Identification of the gene that, when mutated, causes the human obesity syndrome BBS4. *Nat. Genet.* **28**, 188–191 (2001).
15. Menco, P. Ultrastructural aspects of olfactory transduction and perireceptor events. *Semin. Cell Biol.* **5**, 11–24 (1994).
16. Dotty, R.L., Marcus, A. & Lee, W.W. Development of the 12-item cross-cultural smell identification test (CC-SIT). *Laryngoscope* **106**, 353–356 (1996).
17. Beales, P.L. *et al.* Genetic interaction of BBS1 mutations with alleles at other BBS loci can result in non-Mendelian Bardet-Biedl syndrome. *Am. J. Hum. Genet.* **72**, 1187–1199 (2003).
18. Badano, J.L. *et al.* Heterozygous mutations in BBS1, BBS2 and BBS6 have a potential epistatic effect on Bardet-Biedl patients with two mutations at a second BBS locus. *Hum. Mol. Genet.* **12**, 1651–1659 (2003).
19. Beales, P.L., Elcioglu, N., Woolf, A.S., Parker, D. & Flinter, F.A. New criteria for improved diagnosis of Bardet-Biedl syndrome: results of a population survey. *J. Med. Genet.* **36**, 437–446 (1999).
20. Katsanis, N. *et al.* Triallelic inheritance in Bardet-Biedl syndrome, a mendelian recessive disorder. *Science* **293**, 2256–2259 (2001).
21. Wong, S.T. *et al.* Disruption of the type III adenylyl cyclase gene leads to peripheral and behavioral anosmia in transgenic mice. *Neuron* **27**, 487–497 (2000).
22. Bakalyar, H.A. & Reed, R.R. Identification of a specialized adenylyl cyclase that may mediate odorant detection. *Science* **250**, 1403–1406 (1990).
23. Goldstein, B.J., Kulaga, H.M. & Reed, R.R. Cloning and characterization of SLP3: a novel member of the stomatin family expressed by olfactory receptor neurons. *J. Assoc. Res. Otolaryngol.* **4**, 74–82 (2003).
24. Graziadei, P.P.C. & Monti-Graziadei, G.A. The Olfactory System: A Model for the Study of Neurogenesis and Axon Regeneration in Mammals 131–153 (Raven, New York, 1978).
25. Rosenbaum, J.L. & Witman, G.B. Intraflagellar transport. *Nat. Mol. Cell Biol.* **3**, 813–825 (2002).
26. Rugarli, E.I. *et al.* Expression pattern of the Kallmann syndrome gene in the olfactory system suggests a role in neuronal targeting. *Nat. Genet.* **4**, 19–26 (1993).
27. Bacon Moore, A.S., Paulsen, J.S. & Murphy, C. A test of odor fluency in patients with Alzheimer's and Huntington's disease. *J. Clin. Exp. Neuropsychol.* **21**, 341–351 (1999).
28. Gervais, F.G. *et al.* Recruitment and activation of caspase-8 by the Huntingtin-interacting protein Hip-1 and a novel partner Hippi. *Nat. Cell Biol.* **4**, 95–105 (2002).
29. Haycraft, C.J., Schafer, J.C., Zhang, O., Taulman, P.D. & Yoder, B.K. Identification of CHE-13, a novel intraflagellar transport protein required for cilia formation. *Exp. Cell Res.* **284**, 251–263 (2003).
30. Signor, D. & Scholey, J.M. Microtubule-based transport along axons, dendrites and axonemes. *Essays Biochem.* **35**, 89–102 (2000).